Organized Semiconducting Nanostructures from Conjugated Block Copolymer Self-Assembly

Ph. Leclère,[†] V. Parente,[†] J. L. Brédas,*[,†] B. François,[‡] and R. Lazzaroni[†]

Service de Chimie des Matériaux Nouveaux, Centre de Recherche en Electronique et Photonique Moléculaires, Université de Mons-Hainaut, Place du Parc 20, B-7000 Mons, Belgium, and Laboratoire de Recherche sur les Matériaux Polymères, CNRS/UPPA Avenue du Président Angot 2, F-64000 Pau, France

Received June 23, 1998. Revised Manuscript Received September 14, 1998

Self-assembly of block copolymers is attractive for nanodevice fabrication because the association of different polymers by covalent bonding and the interplay between the sequences allows one to generate a variety of structures with well-defined shapes. We present a straightforward approach to generate self-organized organic semiconducting nanostructures. This approach is based on the spontaneous molecular organization of block copolymers containing one fully conjugated segment associated with a nonconjugated sequence. Such systems show high local contrast in their properties and are of interest for applications in nanoscale patterning for quantum confinement of light emission or fabrication of nanowire networks.

1. Introduction

The technological importance of block copolymers stems directly from the phase separation they show on the nanometer scale. The various morphologies resulting from the phase separation have been described in detail for materials in which the components are made of flexible chains ("coil−coil" systems).[1] However, the presence of segments with different stiffness ("rod−coil" block copolymers)[2] or the formation of intermolecular hydrogen bonds or ionic interactions[3] have recently been shown to induce new kinds of morphologies, the formation of which is not completely understood yet. In the present work, we build on the stiffness asymmetry between a fully conjugated chain and a nonconjugated thermoplastic segment to generate a novel morphology where there appear ribbons of the conjugated semiconducting material that are isolated from each other by a insulating thermoplastic matrix.

A number of semiconducting polymers, including polyparaphenylene, polythiophene, and polyacetylene, can be inserted into block copolymers, mainly via living polymerization processes;[4] such reactions allow for strict control of the chain length of each sequence. It is the low polydispersity index combined with immiscibility between the different segments that triggers well-defined microdomain morphologies. In this study, we focus on diblock copolymers containing a fully conjugated polyparaphenylene (PPP) segment, and either a poly(methyl methacrylate) (PMMA) or polystyrene (PS) block; the choice of these thermoplastic polymers is justified by the processability and relatively high working temperature (i.e., up to 100 °C) for potential applications.

Scheme 1

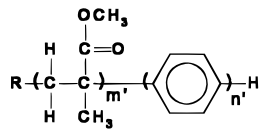

PMMA-PPP

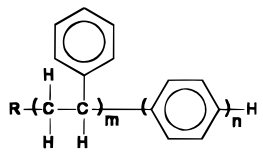

PS-PPP

2. Experimental Section

The PMMA−PPP and PS−PPP block copolymers were prepared, by previously described methods,[4] from precursor copolymers containing PMMA or PS and poly-1,3-cyclohexadiene (PCHD) (see Scheme 1). The precursors are synthesized by anionic polymerization with a lithium counterion in a nonpolar medium. This method affords excellent control of the molecular weights and of the 1,4-binding of the resulting cyclohexene units; the PPP block is then obtained by dehydrogenation of the PCHD sequence. The dehydrogenation process was controlled by solution ^{1}H NMR. The band of vinylic hydrogens completely vanishes after reaction, but the

* Author to whom correspondence should be sent. Telephone: 32-65-37-3356. Fax: 32-65-37-3366. E-mail: jeanluc@averell.umh.ac.be.
[†] Service de Chimie des Matériaux Noureaux.
[‡] Laboratoire de Recherche sur les Matériaux Polymères.

(1) Riess, G.; Bahhadur, P. In *Encyclopedia of Polymer Science and Engineering*, Mark, H. F.; Bikales, N. M.; Overberger, C. G.; Menges, G., Eds.; Wiley: New York, 1989. Bates, F. S.; Fredrickson, G. H. *Annu. Rev. Phys. Chem.* **1990**, *41*, 525.
(2) Chen, J. T.; Thomas, E. L.; Ober, C. K.; Mao, G.-P. *Science* **1996**, *273*, 343. Radzilowski, L. H.; Stupp, S. I. *Macromolecules* **1994**, *27*, 7747. Radzilowski, L. H.; Carragher, B. O.; Stupp, S. I. *Macromolecules* **1997**, *30*, 2110. Chen, X. L.; Jenekhe, S. A. *Macromolecules* **1996**, *29*, 6189. Jenekhe, S. A.; Chen, X. L. *Science* **1998**, *279*, 1903.
(3) Ruokolainen, J.; Mäkinen, R.; Torkkeli, M.; Mäkelä, T.; Serimaa, R.; ten Brinke, G.; Ikkala, O. *Science* **1998**, *280*, 557.
(4) Krouse, S. A.; Schrock, R. R. *Macromolecules* **1988**, *21*, 1885. François, B.; Zhong, X. F. *Synth. Met.* **1991**, *41*−*43*, 955. Widawski, G.; Rawiso, M.; François, B. *J. Chim. Phys.* **1992**, *89*, 1331. Widawski, G.; Rawiso, M.; François, B. *Nature* **1994**, *369*, 387. François, B.; Widawski, G.; Rawiso, M.; Cesar, B. *Synth. Met.* **1995**, *69*, 463.

10.1021/cm980445a CCC: $15.00
Published on Web 11/26/1998

formed aromatic H are not visible due to the aggregation of PPP sequences. The presence of chlorine in the elemental analysis reveals some defects due to the fixation of about one chloranil molecule per 20 monomer units in the PPP chain.[5] Thin films, typically 400 nm thick, are deposited on silicon or mica substrates by solvent casting from toluene solutions containing 1 mg/mL of the compounds. After drying in air, the films are annealed at 150 °C for 48 h in a vacuum (10^{-7} T). This temperature is higher than the glass transition temperature of the thermoplastic components (T_g PS = 105 °C; T_g PMMA = 125 °C).

The optical, electrical, and mechanical properties of thin solid films of these rod-coil materials intimately depend on the morphology on the microscopic scale. To rationalize the molecular organization in such block copolymers, an original approach is required that here combines the experimental morphological data obtained from microscopic techniques with information on the chain assembly derived from theoretical calculations on model systems. Atomic force microscopy (AFM) and related techniques are thus used to investigate the surface morphology of these materials. Surface morphology can be best observed when the AFM apparatus is operated in tapping-mode (TM),[6] and the phase of the oscillation of the cantilever interacting with the surface is measured and compared with the phase of the exciting signal; this mode of operation is referred to as phase detection imaging (PDI) and is very sensitive to the local mechanical properties of the surface.[7,8] AFM images were recorded with a Nanoscope IIIa microscope operated at room temperature in TM in air (TMAFM), using microfabricated cantilevers (spring constant of 30 Nm^{-1}). The images were made with the maximum available number of pixels (512) in each direction and are shown as captured. The influence of the conjugated segment on the morphology is analyzed as a function of chain composition. Molecular dynamics calculations allow us to interpret the shape and size of microdomains observed on the surface in terms of molecular aggregation. The molecular dynamics simulations have been performed with the Cerius2 package developed by Molecular Simulations Inc. The potential energy of each system is described with the Universal Force Field using partial atomic charges set to zero. The simulations rely on to both NVT and NPT ensembles for nonperiodic and periodic systems, respectively; temperature is set at 300 K, and the dynamics runs last for 100 ps with steps of 1 fs.

3. Results

Figure 1 shows the PDI images recorded by TMAFM for copolymers with varying PPP contents: (a) 91:9, PS/PPP (w/w) and (b) 80:20, PMMA/PPP (w/w). The corresponding topographic images (not shown here) show a smooth surface with a root-mean square roughness of a few nanometers (σ_{rms} = 2−3 nm) over a 1 × 1 μm^2 area. The PDI images obtained simultaneously with and on the same area as the topographic data are made of a distribution of dark, elongated objects in a brighter matrix. Because PS (or PMMA) and PPP possess rather different mechanical properties, on the basis of the weight ratio of the two components and recently proposed mechanisms of contrast formation in PDI-AFM,[9,10] the contrast in Figure 1a[1b] can be assigned

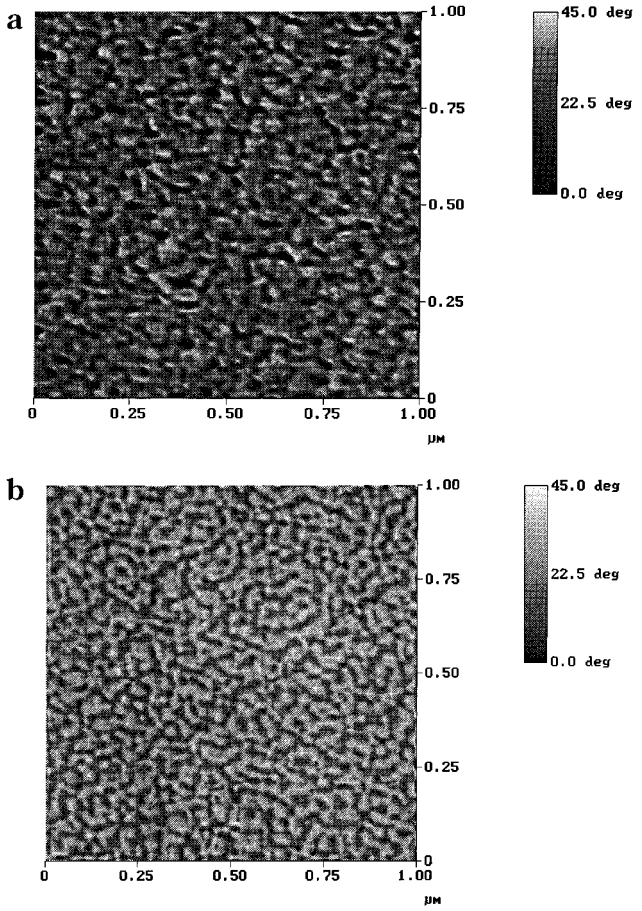

Figure 1. Atomic force microscopy phase detection images (1 × 1 μm^2) of block copolymers (a) PS−PPP, 91:9 mass ratio (corresponding to 30 000−3000 Da); (b) PMMA−PPP, 80:20 mass ratio (corresponding to 8000−2000 Da).

to *phase-separated microdomains* of PPP and PS [PMMA] segments, the latter constituting the bright matrix and the former forming the dark, elongated structures. In the 91:9 composition range, the morphology of "coil−coil" block copolymers normally consists of spheres of the minor component into a matrix of the major component, whereas for contents ranging from 15 to 35%, a "cylinder in a matrix" morphology is usually observed. Clearly, the image in Figure 1a does not show a distribution of spheres, but Figure 1b is closer to the expected morphology. "Rod−coil" copolymers, such as those studied here, are expected to present specific morphologies as well as shifts in the compositions for which transitions between ordered phases (i.e., spheres to cylinders to lamellae) occur.[11] The difference in stiffness between the components, which has been shown to influence the phase behavior of "rod−coil" systems,[12] is an essential aspect of our copolymers; varying the nature of the nonconjugated sequence (hence, its flexibility) therefore provides control of the relationship between the copolymer composition and the phase morphology diagram. Note also that because PS

(5) Zhong, X. F.; François, B. *Makrol. Chem.* **1991**, *192*, 2277.
(6) Magonov, S. N.; Whangbo, M.-H. *Surface Analysis with STM and AFM: Experimental and Theoretical Aspects of Image Analysis*; VCH: Weinheim, 1996.
(7) Leclère, Ph.; Lazzaroni, R.; Brédas, J. L.; Yu, J. M.; Dubois, Ph.; Jérôme, R. *Langmuir* **1996**, *12*, 4317.
(8) Zhong, Q.; Inniss, D.; Kjoller, K.; Elings, V. B. *Surf. Sci.* **1993**, *290*, L688. Magonov, S. N.; Elings, V.; Whangbo, M.-H. *Surf. Sci.* **1997**, *375*, L385.
(9) Bar, G.; Thomann, Y.; Brandsh, R.; Cantow, H.-J.; Whangbo, M.-H. *Langmuir* **1997**, *13*, 3807.
(10) Burnham, N. A.; Behrend, O. P.; Oulevey, F.; Gremaud, G.; Gallo, P.-J.; Gourdon, D.; Dupas, E.; Kulik, A. J.; Pollock, H. M.; Briggs G. A. D. *Nanotechnology* **1997**, *8*, 67.
(11) Saunders: R. S.; Cohen, R. E.; Schrock, R. R. *Macromolecules* **1991**, *24*, 5599.
(12) Bates, F. S.; Schulz, M. F.; Rosedale, J. H. *Macromolecules* **1992**, *25*, 5547. Halperin, A. *Macromolecules* **1990**, *23*, 2724. Schweizer, K. S. *Macromolecules* **1993**, *26*, 6050.

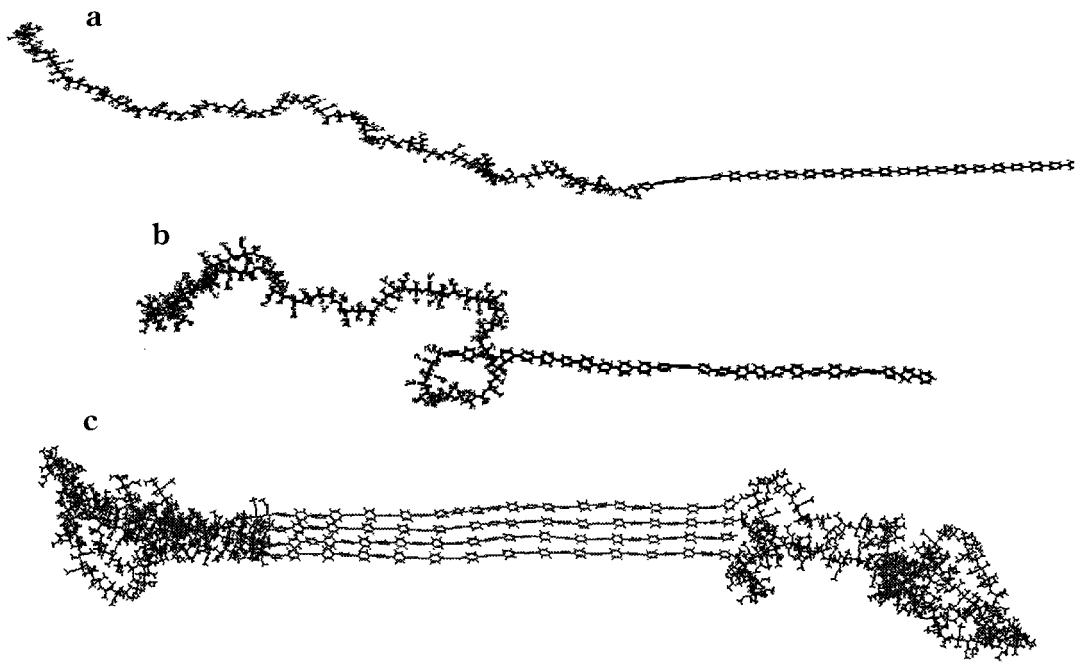

Figure 2. (a) Conformation of a $(MMA)_{80}-(PP)_{26}$ chain in which the PMMA segment, on the left part of the chain, is extended. (b) Conformation of a $(MMA)_{80}-(PP)_{26}$ chain, as obtained with molecular dynamics simulation after 100 ps; the PMMA segment is coiled, whereas the PPP segment remains fully rigid. (c) Conformation of four $(MMA)_{80}-(PP)_{26}$ chains, as obtained with molecular dynamics simulation, illustrating the stacking of the PPP segments and the partial coiling of the PMMA segments.

and PPP are apolar, surface enrichment in one component is not expected; the morphology observed on the surface should thus be similar to the organization in the bulk. In the case of PMMA−PPP, the difference in polarity might induce an increased presence of PPP at the surface; this result is consistent with the fact that dark domains of PPP represent up to 30% of the surface area.

In our case, the PPP segments tend to closely pack in a parallel fashion. This kind of packing is most unlikely to produce spheres or elongated cylinders; instead, it would result in lamellae or ribbons. Therefore, the width of the PPP domains found on the AFM images appears to correspond to the actual width of lamellae (arranged perpendicularly to the surface) or ribbons, rather than to the diameter of cylinders. Because AFM data only reveal the surface morphology, we are not able to determine the extension of the PPP domains toward the bulk; that is, to distinguish between ribbons and lamellae. However, for such low PPP contents (10−20%), it is unlikely that a lamellar structure can develop. The observed morphology should thus correspond to short (Figure 1a) or longer interconnected (Figure 1b) ribbons of PPP in the thermoplastic matrix.

We now turn to a discussion of the molecular arrangement within those ribbons, by combining AFM data and the results of molecular dynamics calculations. The charge transport and optical properties of conjugated materials are directly related to the molecular arrangement in the solid. Determining the orientation and packing of the chains in the microdomains, especially for the conjugated sequences, is therefore important to assess the anisotropic character of such properties in this kind of system.

Although the length and orientation of the dark domains (in Figure 1b) appear to be rather variable, their width is constant at around 12 nm (as measured directly on the images) over the whole surface. A two-dimensional power spectral density analysis[13] of the PDI images provides a typical correlation length of 35 nm corresponding to the average distance between the centers of domains of the same nature, thus representing the sum of typical sizes of PPP and PMMA domains. On this basis, a characteristic size of 23 (i.e., 35−12) nm can be estimated for the PMMA domains. Because the correlation between dark domains is expected to be strongest in areas where the elongated objects are parallel to each other, the 23 nm value should represent the average width of the PMMA domains (i.e., their shortest dimension). In that particular copolymer, the molecular weight of the PPP blocks (2000 Da) corresponds to an average of 26 phenylene units per chain, hence a length of 11.2 nm, which is very close to the AFM-measured width of the PPP domains (12 nm). Because the PPP segment is very rigid and does not fold (vide infra), this indicates that there is only one PPP chain across the PPP domains. It is important to note that very recent neutron scattering experiments performed on similar block copolymers in solution show the presence of ribbonlike domains of the conjugated materials that are one chain wide; this result is fully consistent with our interpretation of the AFM results.[14]

To further analyze the dimensions of the PPP and PMMA segments in terms of molecular arrangement, we have performed canonical molecular dynamics simulations on model systems for the copolymers. Figure 2 shows results obtained on $(MMA)_{80}-(PP)_{26}$ chains, corresponding to the copolymer imaged with AFM in Figure 1b. Figure 2a represents the situation in which a single copolymer chain is forced to be fully extended; the lengths of the PPP and PMMA segments are 11.2

(13) Dumas, Ph.; Bouffakhreddine, B.; Amra, C.; Vatel, O.; Andre, E.; Galindo, R.; Salvan, F. *Europhys. Lett.* **1993**, *22*, 717.
(14) Mignard, E.; François, B, to be published.

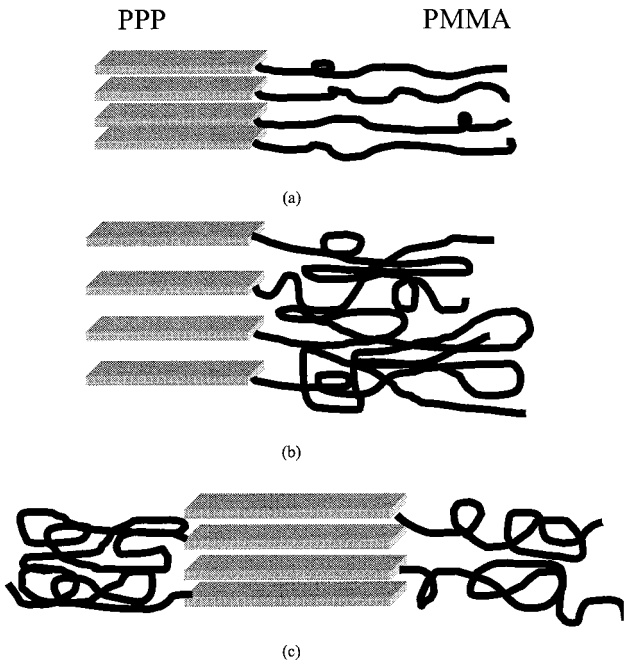

Figure 3. Schematic representation of the molecular arrangement of PMMA−PPP chains: (a) fully extended conformation; (b) head-to-tail arrangement with coiled PMMA segment; and (c) interdigitated arrangement of chains.

and 15 nm, respectively. The simulation performed on an isolated chain (Figure 2b) clearly shows that the behaviors of the two blocks of the copolymer are dramatically different: the PPP segment remains fully extended whereas the PMMA segment tends to coil, with an end-to-end distance reducing from 15 to 7 nm. This situation underlines the rigid character of PPP, which favors parallel packing with other similar segments.[15] This packing is confirmed in Figure 2c, which shows the results of a simulation on four interdigitated copolymer chains; in the final conformation, the PMMA blocks have relaxed and are partially coiled and the PPP segments are closely packed. The arrangement within the PPP domain is similar to the structure observed in polyparaphenylene, with intrachain twists between adjacent phenylene rings of about 30°,[16] and interchain distances of 3.6 to 3.9 Å. The two PMMA domains are characterized by an average individual length of 12 nm.

Combining these theoretical results with the AFM data, we can deduce the molecular arrangement in the copolymer. Three structures can be proposed, in which the PPP domains are one chain wide (Figure 3). In the first one (Figure 3a), the PPP chains are closely packed and all the PMMA segments are arranged similarly in a fully extended conformation. This configuration would lead to a width of about 15 nm for the PMMA domains, as determined from Figure 2a; this value does not match the measured width (23 nm). In fact, PMMA segments spontaneously tend to coil, for entropic reasons. Considering a head-to-tail arrangement of chains with coiled PMMA blocks leads to a very loose packing of the PPP blocks (Figure 3b), which is in contradiction to the theoretical results that indicate that close packing is much favored. The only arrangement that allows both coiling of PMMA and close packing of PPP is the interdigitated organization of Figure 3c. The latter thus represents the best model for the structure of the actual system.

A major aspect to stress is that this type of arrangement, with all PPP segments parallel and facing each other is fundamentally different from the "herringbone" organization typically observed in the crystal structure of oligomers and polymers. It thus suggests that *the presence of the coiled PMMA segments can induce changes in the packing of PPP chains*. Such a parallel, face-to-face arrangement of the conjugated chains is an important structural feature since it is expected to favor charge transport within individual PPP microdomains.

Copolymers with lower PPP contents are likely to show a similar molecular arrangement. The measured width of the PPP domains in the 91:9 (30 000−3000 Da) PS−PPP system is around 15 nm, which is consistent with the value expected for a PPP chain with 39 phenylene rings (16.9 nm). Because PS segments also coil significantly, as confirmed by molecular dynamics calculations, interdigitation of the PPP chains is also expected to take place for those compositions.

4. Conclusions

Thus, the combination of PDI in TMAFM and molecular dynamics simulations allows us to grasp the basic features of the morphology of block copolymers containing a single conjugated segment. The stiffness of the conjugated backbone induces parallel packing of the conjugated chains, which in turn strongly influences the microdomain morphology. For compositions ranging from 10 to 20 mass % in the conjugated material, the AFM data indicate the formation of one-chain-wide ribbons of conjugated chains, surrounded by partially coiled nonconjugated segments.

A major consequence of these results is to open the exciting possibility of fabricating organic semiconducting nanostructures[17] with a controlled shape via an appropriate chemical synthesis:

- systems with a very low content in conjugated materials (e.g., 10%) give rise to nanostructures mostly isolated from each other, reminiscent of quantum dots;
- increasing the amount of conjugated chains to around 20% produces longer ribbons, which could be aligned with an electric field[18] into networks of nanometer-size wires. These systems are thus especially attractive for studies of phenomena such as exciton confinement or charge transport along individual stacks.

Acknowledgment. We are grateful to Ph. Dubois and S.I. Stupp for stimulating discussions. Research on conjugated materials in Mons is supported by the Belgian Federal Government Office of Science Policy (SSTC) "Pôle d'Attraction Interuniversitaire en Chimie Supramoléculaire et Catalyse Supramoléculaire" (PAI

(15) Hässlin, H. W.; Rieckel, C. *Synth. Met.* **1982**, *5*, 37.
(16) Elsenbaumer, R. L.; Shacklette, L. W. In *Handbook of Conducting Polymers*, Skotheim, T. A., Ed.; Marcel Dekker: New York, 1986. Resel, R. *Thin Solid Films* **1997**, *305*, 232.
(17) Romero D. B.; Schaer, M.; Staehli, J. L.; Zuppiroli, L.; Widawski, G.; Rawiso, M.; Francois, B. *Solid State Commun.* **1995**, *95*, 185. Romero, D. B. *Opt. Eng.* **1995**, *34*, 1987.
(18) Amundson, K.; Helfand, E.; Quan, X.; Smith, S. D. *Macromolecules* **1993**, *26*, 2698. Amundson, K.; Helfand, E.; Quan, X.; Smith, S. D. *Macromolecules* **1994**, *27*, 6559. Morkved, T. L.; Lu, M.; Urbas, A. M.; Ehrichs, E. E.; Jaeger, H. M.; Mansky, P.; Russell, T. P. *Science* **1996**, *273*, 931.

4/11), the Government of the Région Wallonne and the European Commission (Project NOMAPOL-Objectif 1-Hainaut), FNRS-FRFC, and an IBM Academic Joint Study. The Mons-Pau collaboration is supported by the Training and Mobility of Researchers program of the European Commission (network SELOA). R.L. is Maître de Recherches du Fonds National de la Recherche Scientifique (FNRS, Belgium).

CM980445A